Applied Radiation and Isotopes 88 (2014) 139–142

Contents lists available at ScienceDirect

Applied Radiation and Isotopes

journal homepage: www.elsevier.com/locate/apradiso

Feasibility study on pinhole camera system for online dosimetry in boron neutron capture therapy

Tatsuya Katabuchi [a,*], Brian Hales [a], Noriyosu Hayashizaki [a], Masayuki Igashira [a], Zareen Khan [a], Tooru Kobayashi [b], Taihei Matsuhashi [a], Koichi Miyazaki [a], Koichi Ogawa [c], Kazushi Terada [a]

[a] Research Laboratory for Nuclear Reactors, Tokyo Institute of Technology, 2-12-1 Ookayama, Meguro-ku, Tokyo 152-8550, Japan
[b] Research Reactor Institute, Kyoto University, Kumatori-cho, Sennan-gun, Osaka 590-0494, Japan
[c] Department of Applied Informatics, Faculty of Science and Engineering, Hosei University, 3-7-2 Kajino-cho, Koganei, Tokyo 184-8584, Japan

AUTHOR-HIGHLIGHTS

- The feasibility of a pinhole camera system for online dosimetry in BNCT was studied.
- A prototype pinhole camera system for online dose imaging for BNCT was built.
- Prompt γ-rays from a phantom irradiated with neutrons were detected.
- The boron-10 reaction rate distribution was reconstructed from the experimental data.

ARTICLE INFO

Available online 31 December 2013

Keywords:
Boron neutron capture therapy
Online dosimetry
Pinhole camera
CdTe detector

ABSTRACT

The feasibility of a pinhole camera system for online dosimetry in boron neutron capture therapy (BNCT) was studied. A prototype system was designed and built. Prompt γ-rays from the $^{10}B(n,\alpha)^{7}Li$ reaction from a phantom irradiated with neutrons were detected with the prototype system. An image was reconstructed from the experimental data. The reconstructed image showed a good separation of the two borated regions in the phantom. The counting rates and signal-to-noise ratio when using the system in actual BNCT applications are also discussed.

1. Introduction

Boron neutron capture therapy (BNCT) has shown the capability to selectively treat tumor cells (Nakagawa et al., 2003; Barth et al., 2005). The high LET particles ($\alpha$and ^{7}Li) emitted from the $^{10}B(n,\alpha)^{7}Li$ reaction terminate tumor cells efficiently. However, in order to transform the BNCT into widely used clinical application, there is a challenge to overcome. In the current procedure, dose evaluation is based on offline analysis and has large uncertainties originating from the evaluation method. Online monitoring of the absorbed dose distribution, in particular, from the $^{10}B(n,\alpha)^{7}Li$ reaction is desired.

Online dosimetry systems based on detecting 478 keV prompt γ-rays from the $^{10}B(n,\alpha)^{7}Li^{*}$ reaction have been proposed (Kobayashi et al., 2000; af Rosenschöld et al., 2006; Minsky et al., 2011; Murata et al., 2011). Most of the proposed online dosimetry imaging systems so far have been parallel multiple hole SPECT (single photon emission computed tomography) systems. Kobayashi et al. (2000) showed a conceptual design of a SPECT system for online monitoring of the distribution of the $^{10}B(n,\alpha)^{7}Li$ reaction rate. The proposed SPECT system consists of a thick tungsten collimator with multiple apertures, and a CdTe detector array. Minsky et al. (2011) built a prototype of a SPECT system using $LaBr_3$(Ce) scintillation detectors, based on a similar collimator design, and demonstrated the first tomographic imaging on borated tumor models in a phantom.

In this study, a different approach from the parallel multiple hole SPECT system was adopted. The feasibility of a pinhole camera system for online dosimetry imaging in BNCT was investigated. A pinhole camera is a type of SPECT system which uses a single cone-shaped collimator (Ogawa et al., 1998). The collimator can be simpler and easier to manufacture than parallel multiple hole collimators. The spatial resolution of the pinhole camera is defined mainly by geometrical distance relationships between the object, the pinhole center and the detector. On the other hand, the spatial resolution of the parallel multiple hole SPECT system is defined by the collimator aperture geometry (diameter, length and distance from the object). This aspect makes the pinhole camera system appealing to a higher

* Corresponding author.
E-mail address: buchi@nr.titech.ac.jp (T. Katabuchi).

0969-8043/$ - see front matter © 2014 Elsevier Ltd. All rights reserved.
http://dx.doi.org/10.1016/j.apradiso.2013.12.026

spatial resolution than that of previous parallel multiple hole systems. Fabrication of small apertures drilled through a thick collimator made up of heavy metal that is necessary for imaging of high energy γ-rays in BNCT application is often very difficult. The achieved spatial resolution of previous BNCT online dose imaging systems was roughly 10 mm. Thus, in general, the pinhole collimator system can easily provide a smaller spatial resolution. We designed and built a prototype of the pinhole camera system for BNCT, and carried out experiments using an accelerator-based neutron source. Prompt γ-rays from a phantom irradiated with neutrons were detected with the prototype system. Image reconstruction from the experimental data was performed. The counting rates and signal-to-noise ratio when using the system in the actual BNCT were also estimated from the experimental results.

2. Experiments

The present pinhole camera system consists of a lead pinhole collimator and a CdTe detector. The pinhole collimator was designed to view a field of 20 cm at a distance of 40 cm from the pinhole center. The thickness of the pinhole collimator was 20 cm. The crystal size of the CdTe detector was 10 mm $\times$ 10 mm $\times$ 1 mm. The CdTe detector was placed just behind the pinhole collimator, at a distance of 10 cm from the pinhole center. The long side of the CdTe detector was aligned to the γ-ray incoming direction such that a high spatial resolution was realized with the short side of 1 mm. From the distance ratio of 10 cm (pinhole–detector) to 40 cm (pinhole–phantom), the spatial resolution of the system is 4 mm. The CdTe detector was mounted on a scanning stage to measure projection images by moving the single detector.

Experiments were performed at the Research Laboratory for Nuclear Reactors at the Tokyo Institute of Technology. Neutrons were generated via the ^{7}Li(p,n)^{7}Be reaction using a 1.9 MeV proton beam from a 3-MV Pelletron accelerator. A cylindrical water phantom (180 mm diam $\times$ 200 mm long) having two tumor models of 30 mm diam $\times$ 50 mm long separated with a gap of 20 mm was irradiated with neutrons from the neutron source. The tumor models contained borated water (2800 ppm ^{10}B). The available neutron flux of the neutron source was approximately three orders of magnitude smaller than the actual BNCT requirements. To get enough count statistics of 0.478 MeV γ-rays, the high concentration of ^{10}B was adopted for the present experiments. The phantom was mounted on a stage to rotate, allowing for measurement of projection images at different rotation angles. A ^{6}Li-glass scintillation detector was placed after the phantom to monitor the incident neutron flux of each run. The pinhole camera system was set on the side of the phantom. In order to shield the system from background γ-rays and neutrons, lead blocks and borated polyethylene blocks were placed around the system. The borated polyethylene blocks were added to the lead shielding as an outer layer. Unwanted 478 keV γ-rays from the borated polyethylene are cut down by the lead inner layer. The distance of the center of the pinhole from the center of the phantom was 30 cm. Projection images of 478 keV γ-rays through the pinhole collimator were measured by moving the CdTe detector. Three phantom rotation angles of 0°, 45° and 90° were chosen for measurements. Background measurement was also made by replacing the phantom with a blank phantom that was a cylindrical water phantom with the same size but did not have tumor models inside.

3. Results and discussion

Fig. 1 shows the pulse height spectra of the detected γ-rays with the CdTe detector. A typical pulse height spectrum for the phantom with tumor models is shown with the background measurement with the no-tumor phantom. Each spectrum was normalized with neutron counts measured with the ^{6}Li-glass detector. A peak of 478 keV γ-rays from the ^{10}B(n, $\alpha\gamma$)^{7}Li reaction is clearly observed only in the spectrum of the tumor model phantom. No 478 keV γ-rays from potential background sources such as borated material for neutron shielding or the neutron target byproduct ^{7}Be which emits 478 keV γ-rays were observed in the background runs. A large peak at 559 keV observed both in the tumor model and the background runs is ascribed to neutron capture events in Cd in the CdTe detector. Insufficient neutron shielding in front of the collimator caused this background.

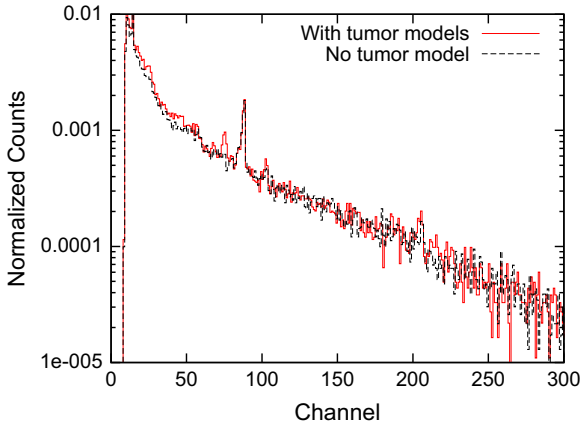

Fig. 1. Pulse-height spectra of the CdTe detector for phantoms with tumor models (red solid line) and no-tumor model (black dashed line). (For interpretation of the references to color in this figure caption, the reader is referred to the web version of this paper.)

It is found that 511 keV annihilation γ-rays, which was expected to be the most problematic background, were not observed. The energy resolution of the CdTe detector at 511 keV was 6 keV in FWHM. This energy resolution is enough to separate the 478 keV peak from the 511 keV annihilation background. Thus, it is unlikely that the annihilation peak overlapped to be indiscernible from the 478 keV peak. Kobayashi et al. (2000) have reported the same observation in their feasibility study using a CdTe detector. The present result supports their claim that 511 keV annihilation background is very small when a small detector like the present detector is used.

Fig. 2 show plots of detected counts of 478 keV γ-rays as a function of distance from the collimator center at phantom rotation angles of 0°, 45° and 90°. The plotted counts were made by subtracting continuum background underneath the peak after normalization with neutron counts of ^{6}Li-glass detector. The indicated errors include only statistical uncertainties. The two borated regions in the phantom are aligned with the pinhole camera axis at a rotation angle of 0°. The projection of the two tumor regions is most separated at 90° and overlap together at 0°. The plots of the detected counts agree with the expectation qualitatively.

We tried to reconstruct the distribution of the ^{10}B(n,α)^{7}Li reaction rate in the phantom from the experimental projection images of detected 478 keV γ-ray counts. The experimental projection data obtained in the experiments were for only the three rotation angles, 0°, 45° and 90°. Assuming system symmetry, the three projection data were used for the other five angles, which are 135°, 180°, 225°, 270° and 315°. Image reconstruction using the Maximum-Likelihood-Expectation-Maximization (ML-EM) algorithm was made from the eight input projection images.

For the image reconstruction, system response to a point source was calculated from simulation using the Monte Carlo simulation code PHITS (Iwase et al., 2002). γ-Rays of 478 keV were